

# Efficient and Mild Carbon Dioxide Hydrogenation to Formate Catalyzed by Fe(II)-Hydridocarbonyl Complexes bearing 2,6-(diaminopyridyl)diphosphine Pincer Ligands.

Federica Bertini,<sup>a</sup> Nikolaus Gorgas,<sup>b</sup> Berthold Stöger,<sup>c</sup> Maurizio Peruzzini,<sup>a</sup> Luis F. Veiros,<sup>d</sup> Karl Kirchner<sup>\*,b</sup> and Luca Gonsalvi<sup>\*,a</sup>

<sup>a</sup> Consiglio Nazionale delle Ricerche (CNR), Istituto di Chimica dei Composti Organometallici (ICCOM), Via Madonna del Piano 10, 50019 Sesto Fiorentino (Firenze), Italy.

<sup>b</sup> Institute of Applied Synthetic Chemistry, Vienna University of Technology, Getreidemarkt 9/163-AC, A-1060 Wien, Austria.

<sup>c</sup> Institute of Chemical Technologies and Analytics, Vienna University of Technology, Getreidemarkt 9/163-AC, A-1060 Wien, Austria.

<sup>d</sup> Centro de Química Estrutural, Instituto Superior Técnico, Universidade de Lisboa, Av. Rovisco Pais No. 1, 1049-001 Lisboa, Portugal.

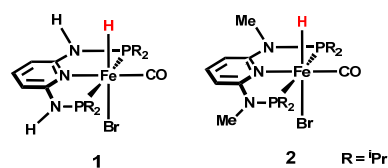
**ABSTRACT:** Fe(II) hydridocarbonyl complexes supported by PNP pincer ligands based on the 2,6-diaminopyridine scaffold were found to promote the catalytic hydrogenation of CO<sub>2</sub> and NaHCO<sub>3</sub> to formate in protic solvents in the presence of bases, reaching quantitative yields and high TONs under mild reaction conditions, with pressures as low as 8.5 bar and temperature as low as 25 °C. NMR and DFT studies highlighted the role of dihydrido and hydridoformate complexes in catalysis.

**KEYWORDS.** CO<sub>2</sub> hydrogenation • iron pincer complexes • homogeneous catalysis • mechanistic studies • DFT calculations.

## INTRODUCTION

The use of CO<sub>2</sub> as a C1-source is a matter of great interest due to its high abundance, availability and low cost. In particular, its reduction to HCOOH or derivatives has attracted significant attention in recent years, since it holds the potential for reversible hydrogen storage.<sup>1</sup> The reduction of NaHCO<sub>3</sub> is also of interest, as CO<sub>2</sub> can be easily trapped in basic solutions and reversible hydrogen storage cycles based on bicarbonate and formate have been proposed.<sup>2</sup> The most efficient catalysts for CO<sub>2</sub> hydrogenation are typically based on expensive noble metals such as ruthenium or iridium.<sup>3</sup> In the quest for cheaper alternatives, the preparation of well-defined earth abundant metal catalysts of comparable activity is highly desirable and important progresses have been made recently.<sup>4</sup> Efficient iron based catalysts supported by tetraphosphine ligands have been reported by Belle<sup>4a,b</sup> and some of us,<sup>4c</sup> whereas Milstein reported that the iron pincer complex [Fe(PNP)(H)<sub>2</sub>(CO)] (PNP = 2,6-bis(di-*tert*-butylphosphinomethyl)pyridine) catalyzes CO<sub>2</sub> hydrogenation at low pressure.<sup>4d</sup> More recently, Hazari and co-workers achieved impressive catalytic activities in Fe-catalyzed CO<sub>2</sub> hydrogenation reaching turnover numbers (TONs) up to 79600 using iron PNP pincer complexes in the presence of Lewis acid (LA) co-catalysts.<sup>4e</sup> In recent years, some of us developed a new class of PNP pincer complexes based on the 2,6-diaminopyridine scaffold where the PR<sub>2</sub> moieties of the PNP ligand are connected to the pyridine ring via NH, N-alkyl or N-aryl spacers.<sup>5</sup> Among these, iron hydrido carbonyl complexes [Fe(PNP<sup>H</sup>-*i*Pr)(H)(CO)(Br)] (**1**) and [Fe(PNP<sup>Me</sup>-*i*Pr)(H)(CO)(Br)] (**2**) shown in Scheme 1 were

shown to be active catalysts for hydrogenation reactions.<sup>5c</sup> Mechanistic studies showed that the N–H spacer of the PNP ligand in **1** can work as a bifunctional catalyst promoting metal-ligand cooperation,<sup>5c,d</sup> while the N–Me spacer in complex **2** prevents such a possibility. In addition, the presence of a labile bromide and strong  $\sigma$ -donating H and CO ligands, could give the ideal donor set suitable for catalytic CO<sub>2</sub> hydrogenation.<sup>4d</sup> Thus, we investigated the activities of these complexes for CO<sub>2</sub> and NaHCO<sub>3</sub> hydrogenation reactions.



**Scheme 1.** Fe-PNP pincer complexes **1** and **2**.

## RESULTS AND DISCUSSION

**Catalytic Studies.** Initially, the catalytic activities of **1** and **2** in NaHCO<sub>3</sub> hydrogenation were tested in different solvents using 0.05 mol% catalyst at 80 °C, 90 bar H<sub>2</sub>, 24 h (Table S1). The best results were obtained in H<sub>2</sub>O/THF (4:1) mixtures which ensure good solubility of both catalysts and substrate, reaching 98% formate yield and TON = 1964 for **1** and 52% formate yield and TON = 1036 for **2**, respectively. In MeOH, TONs and yields decrease by ca. 50% with both catalysts, whereas the reaction does not proceed in neat THF indicating the need of a protic solvent. In all cases, **1** performed better than **2** under analogous conditions (see SI for details). Based on the solvent screening results, the hydrogenation of NaHCO<sub>3</sub>

in H<sub>2</sub>O/THF was then studied with **1** under different conditions of temperature, pressure and catalyst loading (Table 1). In the presence of only 0.005 mol% of **1**, TONs up to 4560 could be achieved at 80 °C, 90 bar H<sub>2</sub> after 24h (entry 2). Either higher or lower temperatures resulted in lower turnover numbers (entries 3,4). Noteworthy, the reaction proceeds *even at room temperature* giving a TON = 188 after 72h (entry 5). Reducing the H<sub>2</sub> pressure resulted in a drop of TONs (entries 6,7), yet at higher catalyst loadings (0.1 mol%) sodium formate was obtained (14% yield) with a TON of 140 at only 8.5 bar H<sub>2</sub> (Milstein's conditions)<sup>4d</sup> after 16h (entry 8).

**Table 1.** Hydrogenation of NaHCO<sub>3</sub> to NaHCO<sub>2</sub> with **1** at different catalyst loadings, temperatures and pressures.<sup>a</sup>

| Entry <sup>a</sup> | Cat. <b>1</b><br>[mol%] | T<br>[°C] | P<br>[bar] | TON <sup>b</sup> | t[h] | Yield <sup>c</sup><br>[%] |
|--------------------|-------------------------|-----------|------------|------------------|------|---------------------------|
| 1                  | 0.05                    | 80        | 90         | 1964             | 24   | 98                        |
| 2                  | 0.005                   | 80        | 90         | 4560             | 24   | 23                        |
| 3                  | 0.005                   | 100       | 90         | 400              | 24   | 2                         |
| 4                  | 0.005                   | 60        | 90         | 2360             | 24   | 12                        |
| 5                  | 0.05                    | 25        | 90         | 188              | 72   | 9                         |
| 6                  | 0.005                   | 80        | 60         | 640              | 24   | 3                         |
| 7                  | 0.005                   | 80        | 30         | 80               | 24   | <1                        |
| 8                  | 0.1                     | 80        | 8.5        | 140              | 16   | 14                        |

<sup>a</sup> General reaction conditions: 20 mmol NaHCO<sub>3</sub>, 0.01 - 0.001 mmol catalyst, 25 mL H<sub>2</sub>O/THF 4:1, 80 °C, 90 bar, 24h. <sup>b</sup> TON = (mmol of formate)/(mmol of catalyst). <sup>c</sup> Yields calculated from the integration of <sup>1</sup>H NMR signals due to NaHCO<sub>2</sub>, using DMF as internal standard.

Next, the hydrogenation of CO<sub>2</sub> to formate in H<sub>2</sub>O/THF (4:1) in the presence of **1** and NaOH as base was studied (Table 2), reaching TONs up to 1220 with nearly quantitative yield under optimized conditions (catalyst/NaOH = 1/1250, CO<sub>2</sub>/H<sub>2</sub> = 40/40 bar, 80°C, 21h).

**Table 2.** Hydrogenation of CO<sub>2</sub> to formate with **1** using different solvents and bases.<sup>a</sup>

| Entry          | Cat. <b>1</b><br>[mol%] | Base             | Solvent              | TON <sup>e</sup> | Yield <sup>f</sup><br>[%] |
|----------------|-------------------------|------------------|----------------------|------------------|---------------------------|
| 1              | 0.08                    | NaOH             | H <sub>2</sub> O/THF | 1220             | 98                        |
| 2 <sup>b</sup> | 0.04                    | NaOH             | H <sub>2</sub> O/THF | 608              | 24                        |
| 3 <sup>c</sup> | 0.008                   | NaOH             | H <sub>2</sub> O/THF | 120              | 1                         |
| 4 <sup>d</sup> | 0.04                    | NaOH             | H <sub>2</sub> O/THF | 656              | 26                        |
| 5              | 0.08                    | DBU              | EtOH                 | 0                | 0                         |
| 6              | 0.08                    | DMOA             | EtOH                 | 0                | 0                         |
| 7              | 0.08                    | NEt <sub>3</sub> | EtOH                 | 288              | 23                        |
| 8              | 0.08                    | -                | EtOH                 | 0                | 0                         |
| 9              | 0.08                    | DBU              | THF                  | 0                | 0                         |

<sup>a</sup> General reaction conditions: 12.5 mmol base, 0.01 mmol catalyst, 25.0 mL solvent, 80 °C, 80 bar total pressure, 21 h. <sup>b</sup> 25.0 mmol base. <sup>c</sup> 0.001 mmol catalyst. <sup>d</sup> 0.005 mmol catalyst. <sup>e</sup> TON = (mmol of formate)/(mmol of catalyst). <sup>f</sup> Yields calculated from the integration of <sup>1</sup>H NMR signals due to NaHCO<sub>2</sub>, using DMF as internal standard.

Higher NaOH/catalyst ratios gave worse results regardless of concentrations (entries 2-4). We then tested the hydrogenation of CO<sub>2</sub> with **1** in EtOH in the presence of different amine bases. Quite surprisingly, formate was not formed using either DBU (1,8-diaza-bicyclo[5.4.0]undec-7-ene) or DMOA (N,N-dimethyloctylamine), whereas in the presence of NEt<sub>3</sub> formate was obtained only in low yields (entries 5-7). The observation that complex **1** fails to catalyze the hydrogenation of CO<sub>2</sub> in EtOH in the presence of amine bases such as DBU or DMOA may be attributed to the fact that EtOH appears to prevent the formation of dihydrides,<sup>5c</sup> which are expected to be the catalytically active species in this reaction. No reaction occurred in EtOH in the absence of base (entry 8), nor in THF with DBU as base due to catalyst decomposition (entry 9).

A complete screening of the effects of catalyst concentration, nature of base, solvent and temperature for CO<sub>2</sub> hydrogenation in the presence of **2** was then carried out (Table 3).

**Table 3.** Hydrogenation of CO<sub>2</sub> to formate with **2** using different solvents and bases.<sup>a</sup>

| Entry               | Cat. <b>2</b><br>[mol%] | Base             | Solvent              | T<br>[°C] | TON <sup>i</sup> | Yield <sup>j</sup><br>[%] |
|---------------------|-------------------------|------------------|----------------------|-----------|------------------|---------------------------|
| 1                   | 0.08                    | NaOH             | H <sub>2</sub> O/THF | 80        | 680              | 54                        |
| 2 <sup>b</sup>      | 0.04                    | NaOH             | H <sub>2</sub> O/THF | 80        | 372              | 15                        |
| 3                   | 0.08                    | NaOH             | MeOH                 | 80        | 220              | 18                        |
| 4                   | 0.08                    | NaOH             | EtOH                 | 80        | 654              | 53                        |
| 5                   | 0.08                    | DBU              | EtOH                 | 80        | 1153             | 92                        |
| 6                   | 0.08                    | DMOA             | EtOH                 | 80        | 452              | 36                        |
| 7                   | 0.08                    | NEt <sub>3</sub> | EtOH                 | 80        | 686              | 55                        |
| 8                   | 0.08                    | -                | EtOH                 | 80        | 0                | 0                         |
| 9                   | 0.08                    | DBU              | THF                  | 80        | 0                | 0                         |
| 10 <sup>c,d</sup>   | 0.1                     | DBU              | EtOH                 | 80        | 480              | 48                        |
| 11 <sup>c</sup>     | 0.1                     | DBU              | EtOH                 | 25        | 856              | 86                        |
| 12 <sup>c,e</sup>   | 0.1                     | DBU              | EtOH                 | 25        | 1032             | 103                       |
| 13 <sup>c,f</sup>   | 0.01                    | DBU              | EtOH                 | 80        | 9840             | 98                        |
| 14                  | 0.01                    | DBU              | EtOH                 | 25        | 465              | 5                         |
| 15                  | 0.005                   | DBU              | EtOH                 | 80        | 10275            | 21                        |
| 16 <sup>c,g</sup>   | 0.001                   | DBU              | EtOH                 | 80        | 5000             | 5                         |
| 17 <sup>c,f,h</sup> | 0.01                    | DBU              | EtOH                 | 80        | 620              | 6                         |
| 18 <sup>a</sup>     | -                       | DBU              | EtOH                 | 80        | 0                | 0                         |
| 19 <sup>k</sup>     | 0.08                    | DBU              | EtOH                 | 80        | 1163             | 93                        |

<sup>a</sup> General reaction conditions: 12.5 mmol base, 0.01 mmol catalyst, 25.0 mL solvent, 21 h. <sup>b</sup> 25.0 mmol base. <sup>c</sup> 10.0 mmol base. <sup>d</sup> 8.5 bar (CO<sub>2</sub>/H<sub>2</sub> = 1:1) total pressure. <sup>e</sup> 72 h. <sup>f</sup> 0.001 mmol catalyst. <sup>g</sup> 0.0001 mmol catalyst. <sup>h</sup> In the presence of LiOTf as Lewis Acid additive, DBU:LiOTf = 7.5. <sup>i</sup> TON = (mmol of formate)/(mmol of catalyst). <sup>j</sup> Yields calculated from the integration of <sup>1</sup>H NMR signals due to NaHCO<sub>2</sub>, using DMF as internal standard. <sup>k</sup> As for <sup>a</sup>, Hg(0) added.

As for NaHCO<sub>3</sub> hydrogenation, catalyst **2** showed poorer performance compared to **1** in the hydrogenation of CO<sub>2</sub> in H<sub>2</sub>O/THF (4:1) in the presence of NaOH (Table 3, entries 1,2 vs Table 2, entries 1,2). Among alcohols, reactions in EtOH gave comparable activity to what observed in H<sub>2</sub>O/THF (entry 4), whereas worse performance was achieved in MeOH (entry 3). Based on the solvent screening results, amine screening

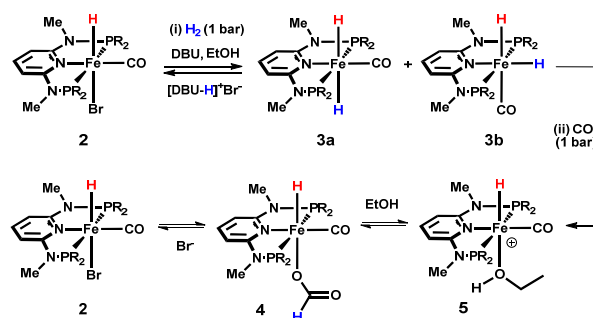
was then studied for CO<sub>2</sub> hydrogenation with **2** in EtOH. To our delight, using DBU as base gave nearly quantitative formate yield (>90%) with a TON of 1153 at 80 °C under 80 bar total pressure (entry 5). Using either DMOA or NEt<sub>3</sub> instead of DBU resulted in lower TONs (entries 6,7) and no reaction occurred in the absence of base (entry 8) or with DBU in THF (entry 9) under otherwise analogous conditions.

The potential of catalyst **2** was then further explored under milder reaction conditions. At first, the effect of lower total pressure was determined. In the presence of 0.1 mol% of **2** a TON of 480 was reached after 21h at 80 °C under only 8.5 bar H<sub>2</sub>/CO<sub>2</sub> (1:1) (entry 10), an activity comparable to that of other known iron pincer catalysts.<sup>4d,f</sup> Then, temperature effects were studied. At 25 °C, catalyst **2** manifested a remarkable catalytic activity, affording sodium formate in high yields<sup>6</sup> with a TON of 856 after 21h and of 1032 after 72h under 80 bar initial pressure (entries 11,12) in the presence of 0.1 mol% catalyst. To the best of our knowledge, these are the highest TONs obtained for Fe-catalyzed CO<sub>2</sub> hydrogenation at room temperature to date.

Finally, the effect of catalyst loading was studied. At lower catalyst loading (0.01 mol%) sodium formate was still obtained in excellent yield (98%) with a TON of 9840 after 21h at 80 °C (entry 13), whereas a TON of 465 was achieved at 25 °C after 21h at 80 bar (entry 14). Reducing further the catalyst loading to 0.005 mol%, CO<sub>2</sub> formate was still achieved with a high TON of 10275 albeit in low yield respect to the base (21%, entry 15). Lowering further the catalyst amount (0.001 mol%) under the same conditions resulted in a lower TON of 5000 (entry 16). We also tested the effect of additives at high substrate to catalyst ratios. Surprisingly, in contrast to what observed by Hazari *et al.*,<sup>4e</sup> the use of a LA co-catalyst such as LiOTf affected negatively the performance (entry 17). Colloidal metal catalysis was ruled out by carrying out Hg poisoning test which gave comparable results to what observed in the original run (entry 19 vs. 5).

**Mechanistic Studies.** In order to gain insights in the reaction mechanism, the reactivity of complex **2** was investigated in stoichiometric reactions by NMR techniques. Exposure of an EtOH solution of **2** to H<sub>2</sub> (1 bar) in the presence of KO<sup>t</sup>Bu resulted in the quantitative formation of dihydrides **3a** and **3b** (*cis* and *trans* isomers).<sup>5c,7</sup> The <sup>31</sup>P{<sup>1</sup>H} NMR spectrum exhibits two singlets at 187.5 ppm (**3a**) and 189.9 ppm (**3b**), while the <sup>1</sup>H NMR exhibits a triplet at -9.57 ppm for **3a** and a broad resonance at -13.86 ppm for **3b**. Upon cooling to -50 °C, the broad signal starts to split into two separate triplets centered at -8.82 ppm and -17.64 ppm.<sup>7</sup> Using DBU as base, NMR analysis revealed that only 40% of **2** was converted into the Fe(II) dihydrides **3**, even after prolonged standing under an hydrogen atmosphere, suggesting that **2** and **3** are in equilibrium with each other (Scheme 2, step i). This may be explained by the lower pK<sub>a</sub> value of [DBU-H]<sup>+</sup> in comparison to tBuOH.<sup>8</sup>

Next, the EtOH/base solution containing *in situ* formed **3** was stirred under an atmosphere of CO<sub>2</sub> for 30 min. Regardless of the base used, we observed the formation of the hydridoformate complex [Fe(PNP<sup>Me</sup>-iPr)(H)(CO)(η<sup>1</sup>-O<sub>2</sub>CH)] (**4**, Scheme 2, step ii) characterized by a triplet at -24.71 ppm for the hydride and a singlet at 7.96 ppm for the proton of the formate ligand, which both integrate to 1 in the <sup>1</sup>H NMR spectrum (see SI).



**Scheme 2.** Stepwise reaction of **2** with H<sub>2</sub> (i) and CO<sub>2</sub> (ii) in the presence of DBU as base in EtOH.

Under these reaction conditions, **4** is in equilibrium with **2** due to the presence of bromide anions in solution. As a result, a broad signal at 8.65 ppm due to free formate salt appeared in the corresponding <sup>1</sup>H NMR spectrum. In addition, the cationic hydride complex [Fe(PNP<sup>Me</sup>-iPr)(H)(CO)(EtOH)]<sup>+</sup> (**5**) was present (Scheme 2), exhibiting a <sup>1</sup>H NMR triplet resonance at -25.57 ppm. The <sup>31</sup>P{<sup>1</sup>H} NMR chemical shift of **5** is very close to that of formate complex **4**. However, no signal for the free formate counteranion could be found in the <sup>1</sup>H spectrum of **5**. Noteworthy, complex **5** was independently synthesized by treatment of **2** with silver salts in EtOH.<sup>7</sup> In a separate experiment, stirring a mixture of **2** and sodium formate (4 equiv.) in EtOH for 1h also affords a mixture of **2**, **4** and **5**. In another experiment, this time starting from *isolated* **3**, the reaction with CO<sub>2</sub> in EtOH afforded **5** with minor traces of **4**. Evidently, the formate ligand is easily displaced by an excess of solvent under these conditions.

Single crystals of **4** suitable for X-ray diffraction analysis were obtained by slow diffusion of pentane into a concentrated solution of the complex in THF under an atmosphere of CO<sub>2</sub>. The solid state structure of **4** confirms the geometry proposed on the basis of NMR data. A structural view is depicted in Figure 1 with selected bond distances given in the caption. Complex **4** adopts a distorted octahedral geometry around the metal center with the formate and hydride ligands *trans* to each other and in *cis* position to the CO ligand. The hydride could be unambiguously located in the difference Fourier maps. The Fe-H distance was refined to 1.46(2) Å.

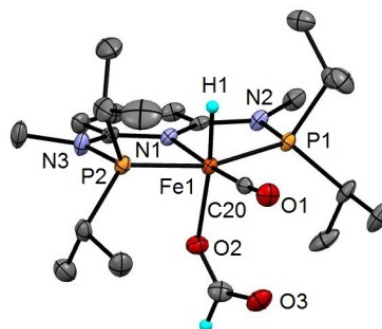
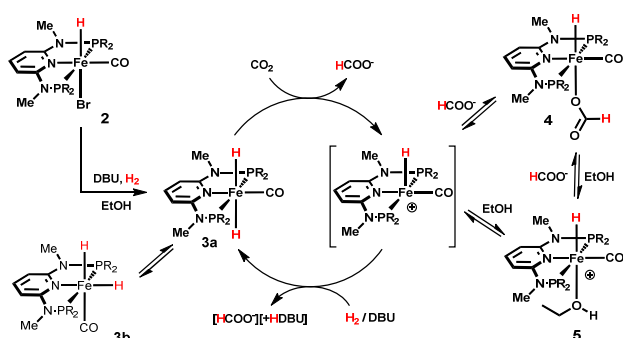


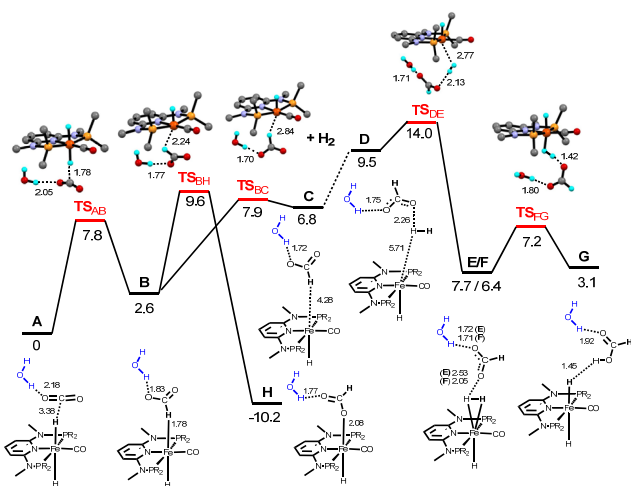
**Figure 1.** Structural view of **4** showing 50% thermal ellipsoids (most H atoms and a second independent complex omitted for clarity). Selected bond lengths (Å) and angles (deg): Fe1-P1 2.1765(7), Fe1-P2 2.1789(7), Fe1-N1 2.004(2), Fe1-C20 1.737(2), Fe1-O2 2.032(2), Fe1-H1 1.46(2), P1-Fe1-P2 162.57(2), N1-Fe1-C20 175.58 (8).

Based on the experimental evidence, a catalytic cycle for CO<sub>2</sub> hydrogenation starting from **2** can be proposed, encompassing formation of dihydrides **3**, CO<sub>2</sub> insertion to give the hydrido formate complex **4** followed by hydrogenolysis and formate elimination giving back **3** in the presence of base. Solvent-assisted formate decoordination in **4** may occur to leave a highly reactive, unobserved pentacoordinate cationic Fe(II) hydridocarbonyl species, which can be stabilized by EtOH coordination to give **5**, observed by NMR (Scheme 3).

Further mechanistic details on CO<sub>2</sub> hydrogenation mechanism were obtained by DFT calculations using **3a** as the initial active species. The free energy profile is shown in Scheme 5. Computational details are presented as SI. The model used in the calculations included one explicit water molecule that provides H-bond stabilization of the intermediates. The highlights of the calculated mechanism are presented in Scheme 4 with relevant intermediates and the corresponding free energy values.<sup>9</sup>



**Scheme 3.** Proposed catalytic cycle for CO<sub>2</sub> hydrogenation with **3a**.



**Scheme 4.** Free energy profile calculated (DFT) for the hydrogenation of CO<sub>2</sub> catalyzed by **3a** (denoted as **A**). The free energy values (kcal/mol) are referred to the initial reactants and relevant distances (Å) are indicated.

In the first step of the calculated mechanism, from **A** to **B**, the hydride attack from complex **3a** to a CO<sub>2</sub> molecule results in a H-bonded formate complex. This is a facile process with a barrier of 7.8 kcal/mol. In the resulting intermediate (**B**) the formate ion is stabilized by a H-bond with the water molecule. From **B**, formate can coordinate the metal giving complex **4** (**H** in Scheme 5), where the formate ligand is bonded through

the O-atom. This intermediate represents the potential well of the mechanism, thus it may be viewed as the catalyst resting state. Alternatively, the formate ion dissociates from the metal in **B** to give **C**, opening one coordination position that is occupied by a molecule of H<sub>2</sub> in the following step. Both processes are competitive with barriers within 2 kcal/mol. The reaction pathway proceeds with H<sub>2</sub> addition to **C** yielding the dihydrogen complex **F**. This process has an energy barrier of 14 kcal/mol, corresponding to the highest of the entire mechanism. In the final step, the formate ion is protonated by **F**, regenerating the initial complex **3a** and producing formic acid. Giving the excess of base present in the reaction medium under experimental conditions, formed acid will be then deprotonated in an acid-base reaction that provides the final driving force for the entire process. Importantly, the free formate ion (the reaction product under the experimental conditions) is stabilized by a H-bond with the nearby water molecule in intermediates **E/F**.<sup>9</sup> This facilitates the opening of the coordination position that will be used by H<sub>2</sub> in the following step of the mechanism, justifying the need of a protic solvent in the catalytic reaction. A similar reaction mechanism was recently proposed for the selective hydrogenation of aldehydes in EtOH with **3** as catalyst<sup>7</sup> and by other authors on related systems.<sup>10</sup>

## CONCLUSIONS

In conclusion, selected Fe(II) pincer-type complexes of 2,6-diaminopyridyl-bis(diisopropylphosphine) gave high activities as catalysts for CO<sub>2</sub> and NaHCO<sub>3</sub> reduction to formate under very mild to moderate conditions, even at room temperature. Mechanistic details were obtained by NMR techniques highlighting the role of dihydride and hydridoformate complexes. DFT calculations indicate an outer sphere mechanism with a hydridoformate complex as catalyst resting state and suggest that the overall reaction is pushed forward by the acid-base reaction between the product (formic acid) and the excess base present in solution. Protic solvents promote catalysis by stabilizing the reaction intermediates and assisting formate elimination from the coordination sphere of the metal.

## ASSOCIATED CONTENT

**Supporting Information.** General materials and methods, synthetic procedures, NMR experiments and spectra, cartesian coordinates of the computed structures, crystallographic data for the X-ray structure of **4**, additional catalytic data. This material is available free of charge via the Internet at <http://pubs.acs.org>.

## AUTHOR INFORMATION

### Corresponding Authors

\* E-mail for L.G.: [l.gonsalvi@iccom.cnr.it](mailto:l.gonsalvi@iccom.cnr.it).

\* E-mail for K.K.: [karl.kirchner@tuwien.ac.at](mailto:karl.kirchner@tuwien.ac.at).

### Author Contributions

All authors have given approval to the final version of the manuscript.

## ACKNOWLEDGMENT

Financial contributions by CNR and ECRF through projects EFOR and HYDROLAB-2.0, respectively, are gratefully acknowledged. This work was also supported by COST Action CM1205 CARISMA (Catalytic Routines for Small Molecule Activation). L.F.V. acknowledges Fundação para a Ciência e

Tecnologia, grant UID/QUI/00100/2013. NG and KK gratefully acknowledge the Financial support by the Austrian Science Fund (FWF) (Project No. P24583-N28).

## REFERENCES

- (1) a) Joó, F. *ChemSusChem* **2008**, *1*, 805–808; b) Enthaler, S.; von Langermann, J.; Schmidt, T. *Energy Environ. Sci.* **2010**, *3*, 1207–1217; c) Loges, B.; Boddien, A.; Gärtner, F.; Junge, H.; Beller, M. *Top. Catal.* **2010**, *53*, 13–14.
- (2) a) Papp, G.; Csorba, J.; Laurency, G.; Joó, F. *Angew. Chem. Int. Ed.* **2011**, *50*, 10433–10435; b) Boddien, A.; Gärtner, F.; Federsel, C.; Sponholz, P.; Mellmann, D.; Jackstell, R.; Junge, H.; Beller, M. *Angew. Chem. Int. Ed.* **2011**, *50*, 6411–6414.
- (3) Wang, W.-H.; Himeda, Y.; Muckerman, J. T.; Manbeck, G. F.; Fujita, E. *Chem. Rev.* **2015**, *115*, 12936–12973.
- (4) a) Federsel, C.; Boddien, A.; Jackstell, R.; Jennerjahn, R.; Dyson, P. J.; Scopelliti, R.; Laurency, G.; Beller, M. *Angew. Chem. Int. Ed.* **2010**, *49*, 9777–9780; b) Ziebart, C.; Federsel, C.; Anbarasan, P.; Jackstell, R.; Baumann, R.; Spannenberg, W. A.; Beller, M. *J. Am. Chem. Soc.* **2012**, *134*, 20701–20704; c) Bertini, F.; Mellone, I.; Ienco, A.; Peruzzini, M.; Gonsalvi, L. *ACS Catal.* **2015**, *5*, 1254–1265; d) Langer, R.; Diskin-Posner, Y.; Leitun, G.; Shimon, L. J. W.; Ben-David, Y.; Milstein, D. *Angew. Chem. Int. Ed.* **2011**, *50*, 9948–9952; e) Zhang, Y.; MacIntosh, A. D.; Wong, J. L.; Bielinski, E. A.; Williard, P. G.; Mercado, B. Q.; Hazari, N.; Bernskoetter, W. *Chem. Sci.* **2015**, *6*, 4291–4299; f) Rivada-Wheleaghan, O.; Dauth, A.; Leitun, G.; Diskin-Posner, Y.; Milstein, D. *Inorg. Chem.* **2015**, *54*, 4526–4538.
- (5) a) Bichler, B.; Glatz, M.; Stöger, B.; Mereiter, K.; Veiros, L. F.; Kirchner, K. *Dalton Trans* **2014**, *43*, 14517–15419; b) de Aguiar, S. R. M. M.; Öztöpcü, Ö.; Stöger, B.; Mereiter, K.; Veiros, L. F.; Pittenauer, E.; Allmaier, G.; Kirchner, K. *Dalton Trans* **2014**, *43*, 14669–14679; c) Gorgas, N.; Stöger, B.; Veiros, L. F.; Pittenauer, E.; Allmaier, G.; Kirchner, K. *Organometallics*, **2014**, *33*, 6905–6914; d) Bichler, B.; Holzacker, C.; Stöger, B.; Puchberger, M.; Veiros, L. F.; Kirchner, K. *Organometallics* **2013**, *32*, 4114–4121; e) Benito-Garagorri, D.; Becker, E.; Wiedermann, J.; Lackner, W.; Pollak, M.; Mereiter, K.; Kisala, J.; Kirchner, K. *Organometallics* **2006**, *25*, 1900–1913; f) Benito-Garagorri, D.; Wiedermann, J.; Pollak, M.; Mereiter, K.; Kirchner, K. *Organometallics* **2007**, *26*, 217–222; g) Benito-Garagorri, D.; Puchberger, M.; Mereiter, K.; Kirchner, K. *Angew. Chem. Int. Ed.* **2008**, *47*, 9142–9145.
- (6) Over-quantitative yields of formate have been reported with DBU as base, see: Hsu, S.-F.; Rommel, S.; Eversfield, P.; Muller, K.; Klemm, E.; Thiel, W. R.; Plietker, B. *Angew. Chem. Int. Ed.* **2014**, *53*, 7074–7078; see also ref. 4e and references cited therein.
- (7) Gorgas, N.; Stöger, B.; Veiros, L. F.; Kirchner, K. *ACS Catal.* **2016**, in press (DOI: 10.1021/acscatal.6b00436).
- (8) pK<sub>a</sub> references: pK<sub>a</sub> for DBU is ca. 11.5–11.9, see: Kaupmees, K.; Trummel, A.; Leito, I. *Croat. Chem. Acta* **2014**, *87*, 385–395; pK<sub>a</sub> for *t*BuOH in water is 17.
- (9) Free energy values obtained at the B3LYP/VDZP level using the GAUSSIAN 09 package. All calculations included solvent effects (THF) using the PCM/SMD model. A full account of the computational details and a complete list of references are provided as SI.
- (10) Yang, X. *Inorg. Chem.* **2011**, *50*, 12836–12843.

Fe(II) hydrido carbonyl complexes supported by PNP pincer ligands based on 2,6-diaminopyridine scaffold promote CO<sub>2</sub> and NaHCO<sub>3</sub> catalytic hydrogenation to formate in the presence of bases and protic solvents, with quantitative yields and high TONs even at room temperature.

